International Journal of Electrical, Electronic and Communication Sciences
ISSN: 2517-9438
Vol:13, No:8, 2019

Design a Fractional Order Controller for Power Control of Doubly Fed Induction Generator Based Wind Generation System

Abdellatif Kasbi, Abderrafii Rahali

***Abstract*—**During the recent years, much interest has been devoted to fractional order control that has appeared as a very eligible control approach for the systems experiencing parametric uncertainty and outer disturbances. The main purpose of this paper is to design and evaluate the performance of a fractional order proportional integral (FOPI) controller applied to control prototype variable speed wind generation system (WGS) that uses a doubly fed induction generator (DFIG). In this paper, the DFIG-machine is controlled according to the stator field-oriented control (FOC) strategy, which makes it possible to regulate separately the reactive and active powers exchanged between the WGS and the grid. The considered system is modeled and simulated using MATLAB-Simulink, and the performance of FOPI controller applied to the back-to-back power converter control of DFIG based grid connected variable speed wind turbine are evaluated and compared to the ones obtained with a conventional PI controller.

***Keywords*—**Design, fractional order PI controller, wind generation system, doubly fed induction generator, wind turbine, field-oriented control.

I. Introduction

THE wind energy conversion into electricity is a very promising operation, knowing that the source is clean, free and abundant in several regions. At the present time, DFIG based variable speed WGS has become the most popular wind turbine type. The choice of such systems is due to several factors, such as the variable speed operation around the synchronism speed imposed by connection grid with reduced mechanical stress, full generated power control capacity and the back-to-back power converters are sized to transit just a fraction of the rated power (about 25% to 30%) which is an economical interest in minimizing cost and reducing power losses [1]-[4].

Development of control strategies for the variable speed wind turbines based on DFIG-generator to achieve high performance is an important task. Literally, three approaches are used in controlling this type of WGS, namely the direct power control (DPC), direct torque control (DTC) and vector control (VC) [5]. This last method is the most appropriate control method as it makes it possible to regulate separately the reactive and active powers exchanged between the WGS and the electrical grid [1]. In most studies, the researchers focus their studies based on VC approach with the classical proportional integrator (PI) controller effectively control the active and reactive powers generated by DFIG-machine as presented in [6]-[9]. The VC approach using classical PI controller is a very attractive solution for controlling the variable speed wind turbines because it has simple practical implementation and is frequently used in the wind turbine industry; and it presents very acceptable performance. However, this approach has some drawbacks that can degrade its performance. Indeed, this control approach has some drawbacks that can degrade its performance. Indeed, in case of unknown disturbances or when the DFIG-machine parameters change during the time, the response of the closed-loop system back may deviate from the desired response [10], [11]. Therefore, sufficient performance covering the total range of disturbances is not easy to reach with a classical PI controller.

In the current paper, a fractional order PI^{δ} controller is developed as an alternative robust control approach to the classical PI controller in order to achieve the control objectives. FOPI controllers have been introduced as an extended form of integer PI controllers with integrator of real order ‘δ’. Such controllers gained considerable attention recently thanks to the flexibility of fractional integral order [12], [13]. Indeed, the fractional order PI^{δ} controller, with the supplementary parameter δ which is the fractional order of the integration action, has an ability to increase system robustness and therefore, improve the system performance [14]. Several design procedures for the FOPI have been suggested in the literature [19]-[21] where the main objective is that such controllers would lead to more precise and robust control performances.

In this study, the design of FOPI is founded on extending the analytical procedure developed in [15], so that the parameters of FOPID controller are tuned based on some frequency-domain design specifications. The designed fractional-order PI^{δ} controller is destined for power control of DFIG-generator based on variable speed wind turbine connected in power grid.

The remainder of this paper is organized as follows: After the introduction, Section II presents the dynamics of the variable speed WGS based on DFIG-machine. It also presents the maximum power point tracking (MPPT) control strategy. The VC approach for powers control of DFIG-machine is introduced in Section III. In Section IV, details of the designing and applying FOPI controllers for power control of DFIG-machine are discussed precisely. Section V presents the

A. Kasbi and A. Rahali are with Laboratory of Electronics, Automatics and Biotechnology, Faculty of Sciences, Moulay Ismaïl University, B.P. 11201, Zitoune, Meknes, Morocco (e-mail: kasbikaabdellatif@gmail.com, aseec1@hotmail.com).

analysis and robust performance evaluation of the proposed FOPI controller in comparison with the classical PI controller by means of real time simulations. Finally the conclusion is made in Section VI.

II. Description and Modeling of DFIG Based WGS

For years, the doubly fed induction machine has been used for variable speed drives [16]. The grid connected configuration for the variable speed WGS with the reduced capacity power converters is the DFIG-machine based wind turbine system, as shown in Fig. 1. In this figure, the stator winding is directly connected to the grid, while the rotor windings are connected to the electrical grid by means of power converters block which formed two bidirectional power converters connected back to back; namely the rotor side converter (RSC) and grid side converter (GSC). These two power converters are separated through the existence of a DC-link capacitor filter between the two, which operate as energy storage in order to keep the DC-link voltage ripple very small.

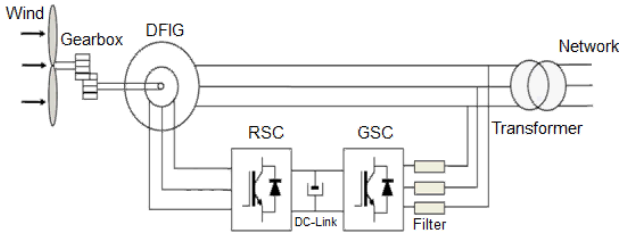

Fig. 1 Configuration of DFIG based wind turbine system

A. Modeling of the Wind Turbine

The aerodynamic power extracted from the wind is expressed in function of the air density ρ [kg/m^2], the blade radius R [m], the wind speed v [m/s] and the power coefficient Cp according to (1):

$$P_{aer} = 0.5\rho S V^3 C_p(\lambda, \beta) \quad (1)$$

where ρ the air density ($\rho = 1.225$ kg/m^{3}at atmospheric pressure), S the surface swept by turbine blades [m^2], V is wind speed [m/s], C_p is power coefficient, λ is tip speed ratio, β the pitch angle [deg], R the blade length[m].

The power coefficient is a nonlinear function of the pitch angle β and tip speed ratioλ. The tip speed ratio is defined as,

$$\lambda = \frac{\Omega_{tur} \cdot R}{V} \quad (2)$$

where Ω_{tur} is the wind turbine angular shaft speed.

As in [6], the expression of the power coefficient C_p as a function of λ and β is given by:

$$C_p(\lambda, \beta) = 0.5176\left(\frac{116}{\lambda_i} - 0.4\beta - 5\right)\exp\left(\frac{21}{\lambda_i}\right) + 0.0068\lambda \quad (3)$$

with:

$$\frac{1}{\lambda_i} = \frac{1}{\lambda + 0.08\beta} - \frac{0.035}{\beta^3 + 1}$$

Once the pitch angle β is maintained fixed at 0°, as shown in Fig. 2, the optimum value of $C_p = C_{p\_max} = 0.48$ (where power extracted is maximal) is reached when $\lambda = \lambda_{opt} = 8.1$.

The mechanical dynamic of the system can be modeled as:

$$J\frac{d\Omega_{mec}}{dt} = C_m - C_{em} - f_v\Omega_{mec} \quad (4)$$

where J represents the system total inertia, f_v is the coefficient of friction, is the electromagnetic torque of DFIG generator, Ω_{mec} (=G. Ω_{tur}) is the mechanical speed of DFIG and C_m is the turbine developed torque ($C_m = C_{aer}/G$ where C_{aer} is the aerodynamic torque).

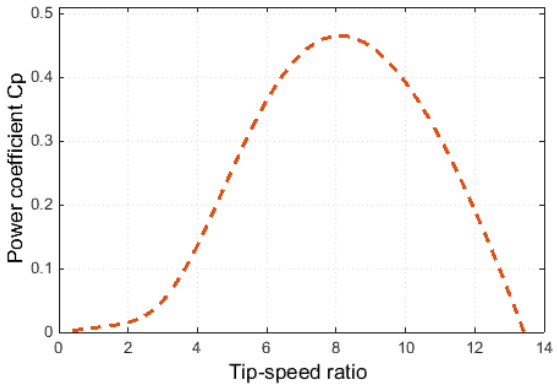

Fig. 2 Power coefficient as a function of λ at β = 0°

B. MPPT Control Strategy

The MPPT control strategy aims to adjust continuously the rotational speed of the DFIG which assures the variable speed operation that maximizes the output power for a wide range of wind speeds. The optimal generator speed corresponds has λopt and β = 0°. At this value, the power coefficient Cp is equal to its maximum value. Thus the electromagnetic torque reference determined by MPPT control strategy is expressed by (5) [17]:

$$C_{em}^{ref} = K_p(\Omega_m^{ref} - \Omega_m) + K_i\int(\Omega_m^{ref} - \Omega_m)dt \quad (5)$$

The MPPT control scheme is shown in Fig. 3.

C. DFIG-Machine Model

The DFIG model in the synchronous (d-q) reference frame can be summarized as follows [4]:

The voltage equations of the stator and rotor windings are defined as:

$$\begin{cases} V_{sd} = R_s I_{sd} + \frac{d\varphi_{sd}}{dt} - \omega_s\varphi_{sq} \\ V_{sq} = R_s I_{sq} + \frac{d\varphi_{sq}}{dt} + \omega_s\varphi_{sd} \\ V_{rd} = R_r I_{rd} + \frac{d\varphi_{rd}}{dt} - (\omega_s - \omega)\varphi_{rq} \\ V_{rq} = R_r I_{rq} + \frac{d\varphi_{rq}}{dt} + (\omega_s - \omega)\varphi_{rd} \end{cases} \quad (6)$$

where ω=p. Ω_{mec} is the electrical speed.

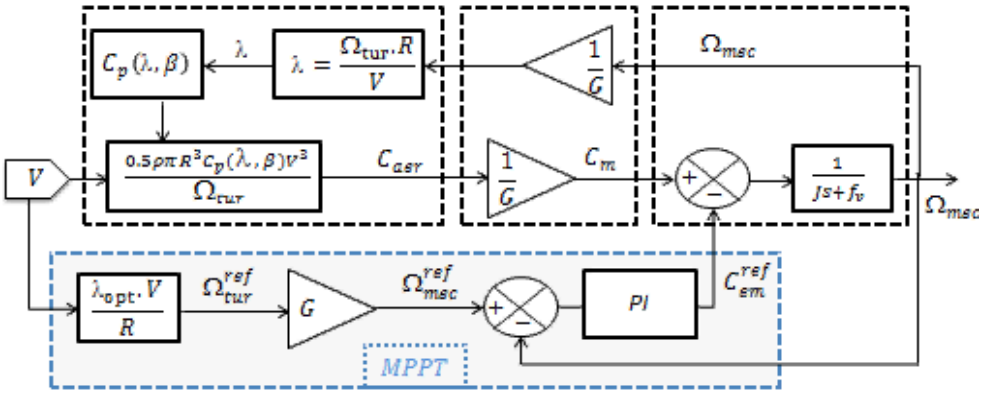

Fig. 3 MPPT based on generator speed control

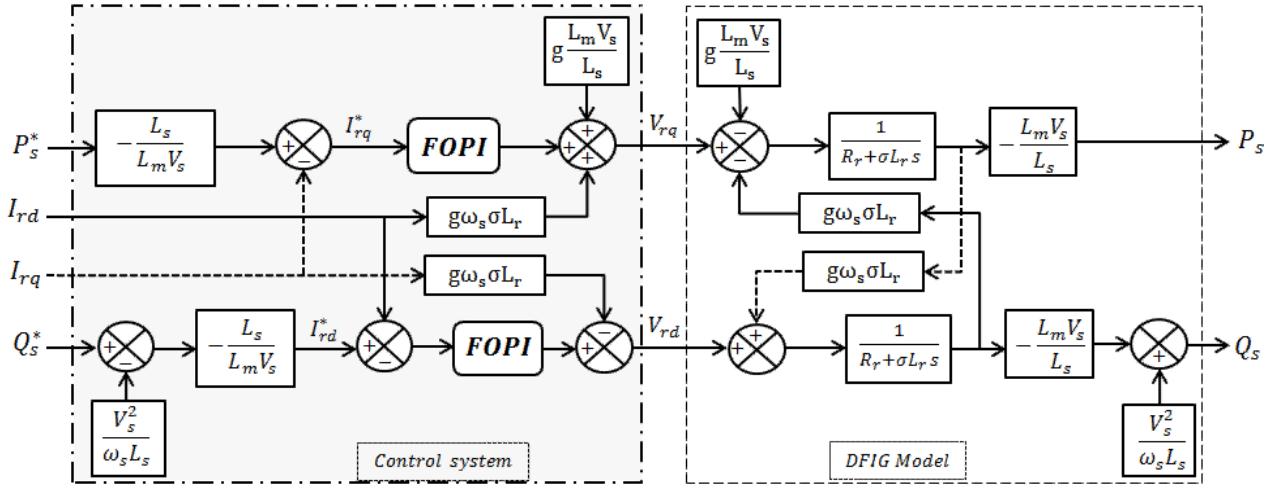

Fig. 4 Schematic diagram of the global control applied to RSC of the DFIG

The stator and rotor flux components in the d-q reference can be written as:

$$\begin{cases} \varphi_{sd} = L_s I_{sd} + L_m I_{rd} \\ \varphi_{sq} = L_s I_{sq} + L_m I_{rq} \\ \varphi_{rd} = L_m I_{sd} + L_r I_{rd} \\ \varphi_{rq} = L_m I_{sq} + L_r I_{rq} \end{cases} \quad (7)$$

The expression of electromagnetic torque C_{em} in a function of components of rotor current and stator flux as:

$$C_{em} = P\frac{L_m}{L_s}\left(I_{rd}\varphi_{sq} - I_{rq}\varphi_{sd}\right) \quad (8)$$

The active and reactive powers are given as follows:

$$\begin{cases} P_s = (V_{sd}I_{sd} + V_{sq}I_{sq}) \\ Q_s = (V_{sq}I_{sd} - V_{sd}I_{sq}) \end{cases} \quad (9)$$

III. DFIG Based Wind Turbine Control Strategy

In this section, we present the philosophy of VC strategy for power control of DFIG based wind turbine. For example, based on the VC strategy, the active and reactive powers, exchanged between the DFIG-generator and grid, are independently controlled in the d and q axes [1]. The idea is to present the model of DFIG in synchronous d-q reference frame.

Aligning the d-axis of reference frame to the stator flux vector and if assuming that the per-phase stator resistance is neglected ($R_s = 0\ ohm$), the voltage and the flux equations of the stator windings can be simplified as [4]:

$$\begin{cases} \varphi_{sd} = \varphi_s \\ \varphi_{sq} = 0 \end{cases} \quad (10)$$

$$\begin{cases} V_{sd} = 0 \\ V_{sq} = \omega_s \varphi_{sd} \end{cases} \quad (11)$$

Using (10) and (11) in (6)-(9) the electromagnetic torque, the rotor voltages and the stator active and reactive power can be expressed in function the rotor currents as follows:

$$C_{em} = P\frac{L_m}{L_s} I_{rq}\varphi_s \quad (12)$$

$$\begin{cases} \mathrm{V_{rd}} = \mathrm{R_s I_{rd}} + \sigma \mathrm{L_r}\frac{\mathrm{dI_{rd}}}{\mathrm{dt}} - \mathrm{g}\sigma\omega_\mathrm{s}\mathrm{L_r I_{rq}} \\ \mathrm{V_{rq}} = \mathrm{R_s I_{rq}} + \sigma \mathrm{L_r}\frac{\mathrm{dI_{rq}}}{\mathrm{dt}} + \mathrm{g}\sigma\omega_\mathrm{s}\mathrm{L_r I_{rd}} + \mathrm{g}\frac{\mathrm{L_m V_s}}{\mathrm{L_s}} \end{cases} \quad (13)$$

$$\begin{cases} P_s = -\frac{V_s L_m}{L_s} I_{rq} \\ Q_s = -\frac{V_s L_m}{L_s} I_{rd} + \frac{V_s \varphi_s}{L_s} \end{cases} \quad (14)$$

where $\sigma = 1 - L_m^2/L_s L_r$ and $g = (\omega_s - \omega)/\omega_s$ is the generator slip.

At this stage, we obtained a model of DFIG in synchronous d-q reference frame and stator flux orientation shows that the active and reactive powers injected in to the grid can be controlled independently. Indeed, the direct component $\mathrm{I_{rd}}$ of the rotor current controls the reactive power while the quadrature component $\mathrm{I_{rq}}$ controls the active power.

The reference rotor currents $\mathrm{I^*_{rd}}$ and $\mathrm{I^*_{rq}}$ are given by:

$$\begin{cases} I^*_{rd} = \frac{V_s}{L_m \omega_s} - \frac{L_s}{L_m V_s} Q^*_s \\ I^*_{rq} = -\frac{L_s}{L_m V_s} P^*_s \end{cases} \quad (15)$$

In the form of two separate loops, the active and reactive powers generated are controlled in the d and q axes. The proposed control system of DFIG-generator based on one FOPI controller for each control loop is shown in Fig. 4.

IV. Design of FOPI Controller

In 1999, Podlubny developed the fractional order $PI^\delta D^\mu$ controller as a generalization of the PID controller using the fractional calculus theory [18], its transfer function is as follows: $K_p + (K_i/s^\delta) + K_d s^\mu$. One of the specialized FOPID controllers is FOPI, where $K_d = 0$ [12], which generalizes in turn the classical PI controller. In the last years, the design procedure of fractional order PI^δ attracts considerable attentions. In this paper, the tuning procedure is based on satisfying a set of the frequency-domain design specifications to achieve the system stability and robustness requirement. If we consider P(s) as the model of the process controlled, then the objective is to get a controller C (s), such that the open loop system G (s) = P(s).C(s) would meet the next design specifications:

- Specification n°1: Gain margin at crossover frequency ω_c condition.

$$|G(j\omega)|_{\omega=\omega_c} = |C(j\omega)P(j\omega)|_{\omega=\omega_c} = 1$$

- Specification $n°$ 2: The phase margin specification is mathematically expressed as:

$$Arg[G(j\omega)]_{\omega=\omega_c} = Arg[C(j\omega)P(j\omega)]_{\omega=\omega_c} = \varphi_m - \pi$$

- Specification $n°$ 3: Robustness to gain variations of the process plant.

$$\frac{d}{d\omega}\,(Arg[\,G(j\omega)])|_{\omega=\omega_c} = 0$$

where ω_c and φ_m are respectively the specific chosen crossover frequency and phase margin for the process plant.

The transfer function of the proposed controller can be described as follows:

$$\mathrm{C(s)} = \mathrm{k_p}\left(1 + \frac{\mathrm{k_i}}{\mathrm{s^\delta}}\right) \quad (16)$$

As shown in Fig. 5, two identical control loops are obtained, one for the direct rotor current i_{rd}, another for the quadrate rotor current i_{rq}.

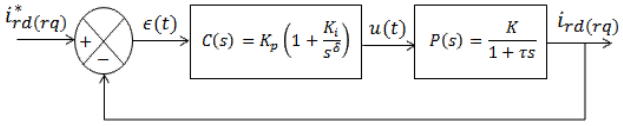

Fig. 5 Loop control of rotor current i_{rd} (i_{rd})

The open-loop transfer function with the FOPI controller for the current loop is

$$G(s) = C(s)P(s) = k_p\left(1 + \frac{k_i}{s^\delta}\right)\frac{k}{1+\tau s} \quad (17)$$

where $k = 1/R_r$, $\tau = \sigma L_r/R_r$ and $s = j\omega$ is the Laplace transform variable.

The open-loop frequency response $G(j\omega)$is that,

$$G(j\omega) = k_p\left(1 + \frac{k_i}{(j\omega)^\delta}\right)\frac{k}{1+j\tau\omega} \quad (18)$$

According to the specification n° 1, the gain of $G(j\omega)$ at ω_c is written by (19):

$$\begin{aligned} &|G(j\omega_c)| = |C(j\omega_c)||P(j\omega_c)| = 1 \Longrightarrow \\ &|G(j\omega_c)| = \left|k_p\left(1 + k_i\, j^{-\delta}\omega^{-\delta}\right)\right|\left|\frac{k}{1+j\tau\omega_c}\right| = 1 \Longrightarrow \\ &\quad kk_p\sqrt{[1 + K_i\omega_c^{-\delta}cos(\delta\pi/2)]^2 + [K_i\omega_c^{-\delta}sin(\delta\pi/2)]^2} = \\ &\qquad \sqrt{1 + [\tau\omega_c]^2}1 \end{aligned} \quad (19)$$

Considering the specification $n°$ 2, the phase of $G(j\omega)$ at crossover frequency ω_c can be expressed as,

$$\begin{aligned} &Arg[G(j\omega_c)] = Arg[C(j\omega_c)] + Arg[P(j\omega_c)] \Longrightarrow \\ &-arctan\frac{K_i\omega_c^{-\delta}sin(\delta\pi/2)}{1+K_i\omega_c^{-\delta}cos(\delta\pi/2)} - \arctan(\tau\omega_c) = \varphi_m - \pi \end{aligned} \quad (20)$$

From (20), we can express K_i in function to fractional integral order δ as,

$$k_i = \frac{-tan[arctan\,(\tau\omega_c) + \varphi_m]}{\omega_c^{-\delta}\sin(\delta\pi/2) + \alpha} \quad (21)$$

where $\alpha = \omega_c^{-\delta}\cos(\delta\pi/2)\,tan[arctan\,(\tau\omega_c) + \varphi_m]$

According to specification n°3 concerning the robustness to gain changes in the plant, we can establish an equation about K_i in the following form:

$$\frac{d}{d\omega}\left(Arg[\,G(j\omega)]\right)|_{\omega=\omega_c} = 0$$
$$= \frac{k_i\delta\omega_c^{\delta-1}\sin(\delta\pi/2)}{\omega_c^{2\delta}+2k_i\omega_c^{\delta}\cos(\delta\pi/2)+k_i^2} - \frac{\tau}{1+(\tau\omega_c)^2} \quad (22)$$

From (22), we can establish another equation regarding the integral gain k_i in the following form:

$$A\omega_c^{-2\delta}k_i^2 + Bk_i + \mathcal{H} = 0 \quad (23)$$

where $A = \frac{\tau}{1+(\tau\omega_c)^2}$ and $B = 2A\omega_c^{-\delta}cos(\delta\pi/2) - \delta\,\omega_c^{-\delta-1}\sin(\delta\pi/2)$. Solving (23) gives,

$$k_i = \frac{-B\pm\sqrt{B^2-4A^2\omega_c^{-2\delta}}}{2A\omega_c^{-2\delta}} \quad (24)$$

Design specifications have been finalized, so a system of three equations of the three variables is obtained. Equations (19) and (21) are from the basic specifications from gain and phase at crossover frequency and the third one (24) is formed to prove the robustness of the controller against the gain variations around ωc. These three equations are solved simultaneously in order to get three parameters k_p, k_i and δ, which are defining the FOPI controller. To proceed for the tuning the parameters defining of the FOPI controller, the gain crossover frequency and the phase margin are considered as: ω_c=500 rad/s, φ_m= 45 degrees.

Out of graphical method, the phase margin specification equation and the equation obtained to confirm the robustness specification are plotted on the same graph and the intersection of the two curves gives the optimal values of k_i and δ, Fig. 6. The value of coefficient of the proportional term k_p is obtained from the third equation (19). Hence, the designed FOPI Controller is,

$$C(s) = 0.055(1+\frac{688}{s^{0.532}}) \quad (25)$$

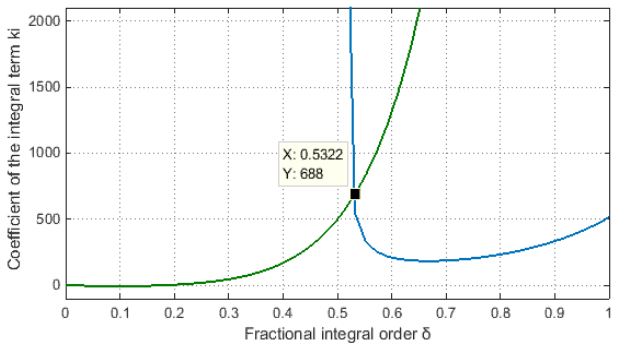

Fig. 6 Relationship curves between k_i and δ.

V. Simulation & Performance Evaluation

To evaluate the performance of the proposed robust FOPI controller in comparison with integer order PI controller which is designed according to the two specifications n°1 and n°2, the DFIG-based variable speed WGS is modeled and simulated under software MATLAB/Simulink. The WGS system standard parameters considered in the simulations are listed in appendix. Fig. 7 describes the wind speed profile applied to the wind turbine during the simulation. The active power reference value is calculated according to the MPPT strategy presented in Fig. 3, while we chose the reactive power reference value of 0 VAR in order to operate at unity power factor. Furthermore, in order to observe the superiority in terms robustness of the FOPI controller compared to the conventional PI controller, a disturbance of random output noise of 5% of the reference signal amplitude is applied on the output of the rotor currents at t = 20 .

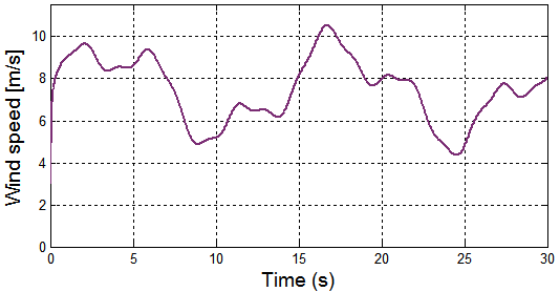

Fig. 7 Wind speed profile

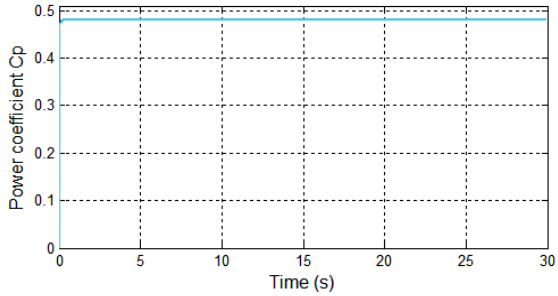

Fig. 8 Power coefficient

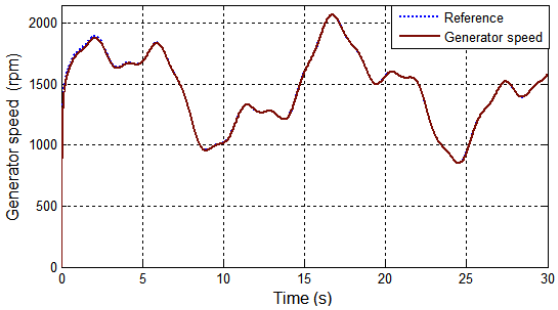

Fig. 9 Generator speed and its optimum reference

Figs. 7-9 expose the time evolution of wind speed, power coefficient and generator speed, respectively. According to

these figures, the MPPT control strategy is valid because the power coefficient remains constant at its maximum value $C_{p\text{-}max} = 0.48$ despite the wind speed variations.

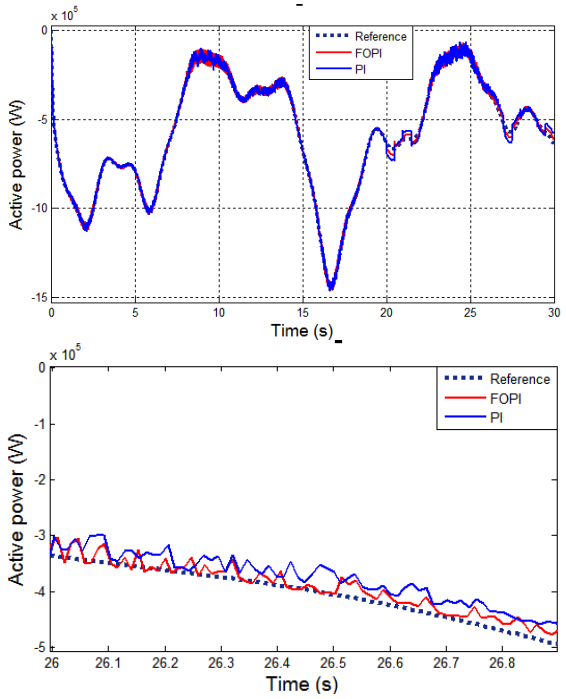

Fig. 10 Active power

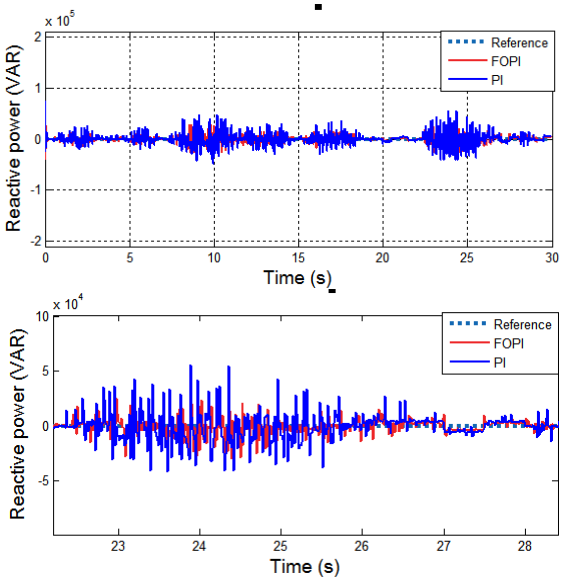

Fig. 11 Reactive power

Figs. 10 and 11 show the active power and reactive power for both controllers, which shows that the proposed FOPI controller has a good tracking performance and also shows its superiority in terms of robustness against disturbances. Therefore, the WGS with the designed FOPI controller has a superior dynamic performance in terms of the tracking reference and the disturbance rejection.

VI. Conclusion

In this paper, a FOPI controller has been designed for power control of DFIG based on variable speed WGS in grid connected. The details of designing and applying FOPI controller for powers control of DFIG-generator are discussed accurately. Indeed, the FOPI controller offers additional tuning flexibility through dint of the additional differentiation order authorizing the improvement of control performance and robustness. Afterwards, the performance of the presented FOPI has been evaluated in terms of reference tracking and robustness against disturbances and it has been compared to the classical PI controller. The simulation results obtained shown that the FOPI controller proposed is more effective in terms of tracking precision, time response and robustness than the integer order PI controller, while it conserves its clarity and simplicity of application.

Appendix

TABLE I
Wind Turbine Parameters

Symbol	Quantity	Value
R	Blade radius	35.25 m
G	Gearbox ratio	90
J	Moment of inertia	1000 kg. m^2
F_{VIS}	Viscous friction coefficient	0.0024 N. M. S^{-1}
V_{in}	Cut-in wind speed	4 m/s
V_{out}	Cut-out wind speed	25 m/s
V_n	Nominal wind speed	16 m/s

TABLE II
DFIG Parameters

Symbol	Quantity	Value
P_n	Rated power	1.5 MW
I_n	Rated current	1900 A
U_{DC}	Rated DC-Link voltage	1200V
f	Stator rated frequency	50Hz
L_s	Stator inductance	0.0137 H
L_r	Rotor inductance	0.0136 H
L_m	Mutual inductance	0.0135 H
R_s	Stator resistance	0.012 Ω
R_r	Rotor resistance	0.021 Ω
p	Number of pair poles	2

References

[1] E. Aydin, A. Polat and L. T. Ergene, "Vector Control of DFIG in Wind Power Applications," in IEEE (ICRERA), Birmingham, Nov. 2016, pp. 478-483.
[2] M. Arghya and C. D. Chatterjee, "Active Power Control of DFIG-Based Wind Farm for Improvement of Transient Stability of Power Systems," IEEE Trans. Power Syst., vol. 31, no. 2, pp. 82-93, February 2015.
[3] L. Xiong, J. Wang, X. Mi and M. W. Khan, "Fractional Order Sliding Mode Based Direct Power Control of Grid-Connected DFIG," IEEE Trans. Power Syst., vol. 33, no. 3, pp. 3087-3096, October 2017.
[4] K. Kerrouche, A. Mezouar and K. Belgacem," Decoupled Control of Doubly Fed Induction Generator by Vector Control for Wind Energy Conversion System," in Overview of renewable energies exploitation in Algeria, Energy Procedia, 2013, vol. 42, pp. 239-248.
[5] R. Errouissi, A. A. Durra, S. M. Muyeen, S. Leng, and F. Blaabjerg, "Offset-free direct power control of DFIG under continuous-time model predictive control," IEEE Trans. Power Electron., vol.32, no. 3, pp.

2265-2277, Mar. 2017.
[6] A. Bakouri, H. Mahmoudi, A. Abbou, “Modelling and Optimal Control of the Doubly Fed Induction Generator Wind Turbine System Connected to Utility Grid,” in Proc. IEEE Int, International Renewable and Sustainable Energy Conference (IRSEC), Marrakech, Morocco, Nov. 2016, pp. 1-6.
[7] T. Brekken and N. Mohan, "A novel doubly-fed induction wind generator control scheme for reactive power control and torque pulsation compensation under unbalanced grid voltage conditions", in: IEEE 34th Annual Power Electronics Specialist Conference, vol. 2, pp. 760–764, June 2003.
[8] T. K. A. Brekken, N. Mohan, “Control of a doubly fed induction wind generator under unbalanced grid voltage conditions", IEEE Transaction on Energy Conversion, Acapulco, Mexico, March 2007, pp.129-135.
[9] M. Machmoum, A. Hatoum and T. Bouaouiche, "Flicker mitigation in a doubly fed induction generator wind turbine system,” Mathematics and Computers in Simulation, vol.81, no.2, pp. 433-445, October 2010.
[10] R. Melcio, V. Mendes and J. Catalo, “Comparative study of power converter topologies and control strategies for the harmonic performance of variable-speed wind turbine generator systems,” Energy, vol.36, pp.520-529, January 2011.
[11] F. E. V. Taveiros, L. S. Barros and F. B. Costa, “Back-to-back converter state-feedback control of DFIG (doubly-fed induction generator)-based wind turbines,”Energy, vol. 89, pp. 896-906, September 2015.
[12] M. S. Tavazoei,”From traditional to fractional PI controller,” IEEE Industrial Electronics Magazine, pp.42-51, Sep. 2012.
[13] R. Hammami, I. Ben Ameur and K. Jelassi, “ Performance Evaluation of fractional order controller for Induction Machine control and comparative study between FOC PI & FOC FOPI,” in IEEE,18th International Conference on Sciences and Techniques of Automatic Control and Computer Engineering (STA), Monastir, Tunisia, 2017, pp. 272-277.
[14] S. Elmetennani, I. N’Doye, K. N. Salama and T. M. Laleg-Kirati, “Performance Analysis of Fractional-Order PID Controller for a Parabolic Distributed Solar Collector,” 2017 IEEE AFRICON, Cape Town, South Africa, 2017, pp. 461-466.
[15] H. S. Li, Y. Luo and Y. Q. Chen,”A Fractional Order Proportional and Derivative (FOPD) Motion Controller: Tuning Rule and Experiments,” IEEE Transactions on control systems technology, vol. 18, no. 2, pp. 516-520, March 2010.
[16] O. P. Bharti, R. K. Saket and S. K. Nagar, “Controller Design For DFIG Driven By Variable Speed Wind Turbine Using Static Output Feedback Technique,” Engineering, Technology & Applied Science Research, vol. 6, no. 4, pp.1056-1061, 2016.
[17] L.M. Fernandez, C.A. Garcia and F. Jurado, “Comparative study on the performance of control systems for doubly fed induction generator (DFIG) wind turbines operating with power regulation,” Energy, vol. 33, pp. 1438–1452, 2008.
[18] I. Podlubny, “Fractional-order systems and PIλDμ-controllers,” IEEE Transactions on Automatic Control, vol. 44, no. 1, pp. 208–214, 1999.
[19] C. Wang, W. Fu, Y. Shi, "An Analytical Design of Fractional Order Proportional Integral Differential Controller for Robust Velocity Servo," 2013 25th Chinese Control and Decision Conference (CCDC), IEEE - 2013, pp. 3359-3362.
[20] C. Y. Wang, Y. Luo, Y. Q. Chen, "An analytical design of Fractional Order Proportional Integral and (Proportional Integral) controllers for robust velocity servo," 2009 4th IEEE Conference on Industrial Electronics and Applications, pp. 329-334.
[21] H. S. Li, Y. Luo and Y. Q. Chen, “A Fractional Order Proportional and Derivative (FOPD) Motion Controller: Tuning Rule and Experiments,” IEEE Transactions on control systems technology, vol. 18, no. 2, pp. 516-520, March 2010.